

Cell Mimetic Liposomal Nanocarriers for Tailored Delivery of Vascular Therapeutics

Samuel I. Mattern-Schain^a, Richard K. Fisher^b, Philip C. West^b, Lauren B. Grimsley^b, Taylor M. Harris^b, Oscar H. Grandas^b, Michael D. Best^{a*}, and Deidra J.H. Mountain^{b*}

^a Department of Chemistry, University of Tennessee, 1420 Circle Drive, Knoxville, TN 37996
e-mail: mdbest@utk.edu
phone: 865-974-8658
Fax: 865-974-9332

^b Department of Surgery, University of Tennessee Graduate School of Medicine, 1924 Alcoa Highway, Knoxville, TN 37920.
e-mail: DMountain@utmck.edu
phone: 865-305-9160
Fax: 865-305-6048

Keywords: Liposomes; Lipids; Drug Delivery; Cell Delivery; Gene Therapy; Fluorescence Microscopy; Imaging

Abstract

Liposomal delivery systems (LDSs) have been at the forefront of medicinal nanotechnology for over three decades. Increasing LDS association to target cells and cargo delivery is crucial to bolstering overall nanodrug efficacy. Our laboratory aims to develop LDSs for molecular therapeutics aimed at vascular pathology. We have previously established a liposome platform that is an effective delivery system for RNA interference in vascular cell types by using polyethylene glycol (PEG) decorated liposomes bearing an octa-arginine (R8) cell penetrating peptide (CPP). Further tailoring liposome membranes to mimic vascular cell membrane lipid constituents may be a promising strategy for increasing cargo delivery. Here we aimed to develop liposomal formulations that could make use of diacylglycerol (DAG) and phosphatidylserine (PS), naturally occurring lipid species that are known to influence vascular cell function, as a facile and efficient means to increase nanodrug efficacy without compromising clinical viability. We investigated the ability of DAG and PS to amplify the cellular uptake of our previously established LDS platform loaded with small interfering ribonucleic acid (siRNA) cargo. Cellular fluorescence microscopy experiments were performed in conjunction with quantitative cell association assays and cytotoxicity assays to analyze the effect of DAG/PS on the differential delivery of fluorescently-tagged liposomes to vascular smooth muscle cells (VSMCs) and vascular endothelial cells

(VECs) and on liposomal-mediated toxicity. In these studies, significant, dose-dependent increases in association to target cells were observed, as well as cell-type specific effects on cell viability. The stability and encapsulation-efficiency of the DAG/PS-modified LDSs were analyzed by standard nanoparticle characterization methods, and siRNA transfection efficacy was quantified to gauge delivery potential as a function of DAG/PS modification. Our results suggest that the signaling lipids tested here imbue our LDS architectures with increased therapeutic potential, without compromising stability, encapsulation efficiency, or biocompatibility, thus presenting a natural strategy to increase nanodrug efficacy and specificity.

1. Introduction

Liposomal delivery systems (LDSs) have remained the premier theranostic nanotechnology since their emergence more than 30 years ago (Alam et al., 2017; Barenholz, 2012; Pattni et al., 2015). When exploring new strategies to increase nanodrug efficacy, researchers often focus on actively targeting their liposomes using peptides (Dicheva et al., 2015) or other molecules (Alam et al., 2017) with affinities for cell surface receptors unique to specific cell types or diseased tissues such as tumors (Saw et al., 2013). Other emerging nanodrug technologies include controlled release liposomes, where vesicles are sensitized to a trigger mechanism that activates drug unloading at the target site. To our knowledge, there is but one actively targeted FDA-approved liposomal nanodrug and none that have triggered release technologies (Bulbake et al., 2017). The factors that impede clinical translatability of advanced nanomedicines is a complex issue that has been previously reviewed (Landesman-Milo and Peer, 2016).

With regard to the delivery of molecular cargo for gene therapeutics, there is ample literature precedent to suggest liposomes designed to carry short interfering ribonucleic acid (siRNA) and other gene-altering species are a viable drug-delivery strategy. At least four different liposomal siRNA-loaded liposomes have made it to clinical trials over the last few years (Kanapathipillai et al., 2014). However, adding functionality to increase delivery and therapeutic efficacy has associated drawbacks. Promising cationic liposomes (CLs) have been developed to enhance cellular delivery of siRNA due to the charge complementarity of cationic liposomes and natural negatively charged cell membrane lipids (Ylä-Herttula and Martin, 2000). However, CLs suffer from poor clinical translatability due to their inherent cytotoxic effects stemming from the utilization of synthetic lipid constituents. Cell penetrating peptides (CPPs) have been widely explored to enhance the cellular uptake of LDSs formed from natural lipid

constituents without the biocompatibility issues that plague CLs, and many inert CPPs have shown promise in laboratory settings. However, no CPP-modified liposomal nanocarriers are available for clinical use to date. Furthermore, liposomal modifications that include polyethylene glycol (PEG) shielding or peptide head-group targeting can lead to lateral dispersion on the membrane surface, which creates bilayer instability. As a result, the percentages of PEG lipids used to shield liposomes and lipopeptides of use for enhancing targeted delivery and cellular entry must be carefully balanced to optimize both circulation time and cargo delivery to specific cell types.

To address these issues discussed, we envisaged the use of naturally occurring lipids diacylglycerol (DAG) and phosphatidylserine (PS) as a facile means for enhancing LDS cell entry while minimizing damage to both liposomes and targeted cells. The LDS presented herein is a CPP-modified neutral liposome we have previously developed as an effective delivery system for siRNA in vascular cells types (Fisher et al., 2017). The long-term goal is to further optimize this LDS as a clinically translatable molecular nanocarrier aimed at the attenuation of peripheral vascular disease (PWD). For this particular investigation, however, our established LDS platform is used for gauging the feasibility and effectiveness of increasing treatment efficacy using DAG/PS. The siRNA cargo utilized here is targeted for silencing of the housekeeping gene glyceraldehyde 3-phosphate dehydrogenase (GAPDH). GAPDH is being used for this discovery-driven LDS development and proof of concept study due to its ease of knockdown evaluation and quantification. Herein, we report the efficacy of DAG and/or PS to potentiate the activity of our LDS to vascular smooth muscle cells (VSMCs) and vascular endothelial cells (VECs) in a cell-type specific manner, while balancing the effect of liposomal-mediated cytotoxicity. DAG and PS have been formed into stable membranes at total percentages as high as 25% (Goldberg et al., 1994) and they do not present bulky headgroups that aggravate the membrane with lateral dispersion forces. We confirm here that these DAG/PS modified liposomes retain their stability and encapsulation profiles, making this a viable strategy for enhancing the efficacy and specificity of LDS for experimental and pre-clinical testing.

2. Materials and methods

2.1. Liposome assembly

All LDS acronyms and compositions are defined in supplementary information Tables S1 and S2. Lipids and cholesterol were purchased from Avanti Polar Lipids (Alabaster, AL, USA). R8-sterate was purchased from LifeTein LLC (Somerset, NJ, USA). Figure 1 illustrates the structure of each lipid

constituent used for LDS formulations. Figure 2 is a schematic representation of experimental LDS groups (PLP, R8, and with and without DAG/PS). All LDS groups were assembled via a modified EtOH injection technique previously described (Fisher et al., 2017). Briefly, lipids were dissolved in CHCl₃, combined as indicated, and dried under N₂ gas to create lipid films. Lipid films were resuspended in 100% molecular grade ethanol and mixed for 60 minutes at 40 °C. Ethanolic lipid solutions were then injected dropwise into 10 mM Tris-HCl (pH 8) with GAPDH siRNA (Thermofisher Scientific, Waltham, MA, USA) at 20:1 weight-to-weight ratio under constant vortexing. Liposomes were then purified from ethanol and unencapsulated siRNA via 24 hour dialysis against PBS at 4°C using 300 kD Float-A-Lyzer™ G2 dialysis devices (Spectrum labs, Rancho Dominguez, CA). Two buffer exchanges during dialysis ensured efficient purification. After dialysis, the final volume was measured and used to determine treatment volumes for experimental assays such that all samples received equimolar lipid or siRNA content. Liposomes were extruded to 100 nm using polycarbonate membrane Nanosizers™ (T&T scientific, Knoxville, TN), stored at 4 °C and used within 48 hours.

2.2. Liposome size and homogeneity characterization

Average size, PDI and zeta potential for every LDS group was measured in triplicate by dynamic light scattering (DLS) and electrophoretic mobility on a Zetasizer Nano ZS instrument (Malvern Instruments Ltd, Worcestershire, UK).

2.3. Liposome encapsulation efficiency

siRNA encapsulation of each preparation was determined using Quant-iT RiboGreen RNA Assay Kit (Thermofisher Scientific). Briefly, 10 µL of liposomes were solubilized in 1% Triton X-100 at 37 °C for 15 min to release encapsulated siRNA from their aqueous cores. Samples were then mixed 1:1 with RiboGreen reagent for fluorescent labeling of siRNA, and emission was then measured at 525 nm. A standard curve of siRNA in 1% Triton X-100 was created to qualify the arbitrary fluorescence units of siRNA released from digested liposomes and thus determine siRNA concentration. Encapsulation efficiency (EE%) was then calculated for each LDS formulation as $(\mu\text{g siRNA encapsulate}/\mu\text{g total siRNA used as assembly}) \times 100$.

2.4. VSMC and VEC culture

Human aortic smooth muscle cells and human aortic endothelial cells were obtained from LifeLine Cell

Technology (Walkersville, MD) as cryopreserved primary cultures of single-donor cells. Cells were grown in T75 flasks and then plated at 1.5×10^5 cells per well (6-well plate) for cytotoxicity, gene expression, and cell association experiments. Cells were grown to 60-80% confluence in VascuLife growth medium composed with VascuLife Basal Medium and either VascuLife smooth muscle cell growth supplement kit or VascuLife endothelial growth supplement kit with gentamicin and amphotericin (LifeLine Cell Technology). Incubation was performed at 37 °C under 5% CO₂ with 95% humidity. Before liposomal treatment, cells were made quiescent by treating overnight with Dulbecco's Modified Eagle Medium (DMEM, ThermoFisher Scientific) with gentamicin and amphotericin.

2.5. Liposomal cell association

Lipid-dependent cell association was measured as previously described (Fisher et al., 2017). Briefly, at ~80% confluence cells were treated with LDS groups at equimolar lipid content of 50uM total lipid in DMEM for 24hr. Cells were washed three times in PBS, lysed with 1 mL of 1% Triton X-100, and centrifuged at 12,000 RPM for 5 min at 4 °C to remove debris. Cell lysates (200 µL) were plated in triplicate in 96-well plates, carefully so as not to contaminate samples with cell debris, and association of rhodamine-labeled liposomes was quantitated within the cell lysates. Fluorometric analysis, performed using a Glomax multi microplate reader with a 575 nm filter (Promega, Madison, WI), determined average fluorescence units for each sample, minus baseline fluorescence of nontreated controls receiving no rhodamine source within each experimental replicate. Samples were normalized to the R8 liposomes to judge fold increase in association as a function of DAG/PS content. Replicate studies always used fresh batches of liposomes. Fluorescence microscopy using a Texas Red fluorescent filter at 400X with 400 ms exposure across all groups provided qualitative representative cell association images using a BX51 Olympus microscope with an Olympus Q-color camera (Olympus Corporation, Shinjuku, Tokyo, Japan).

2.6. Liposomal-mediated cytotoxicity assays

At ~60% confluence, cells were treated with LDS groups at equimolar lipid content of 50uM total lipid in DMEM for 24hr. LIVE/DEAD® Viability/Cytotoxicity Kit (ThermoFisher Scientific) was used to determine relative cell toxicity, according to the manufacturer's instructions. Briefly, DMEM was removed, cells were washed twice in PBS, and co-stained with calcein-AM + ethidium homodimer (1uL

each /1ml PBS) for 15min at 37°C. Stained cells were visualized via fluorescein isothiocyanate (FITC; live) and Texas Red (dead) fluorescent filters. Images were acquired on both filters at 400x, using the same image acquisition system described above, in three independent fields per sample. Cells were counted using ImagePro software (Media Cybernetics, Inc., Rockville, MD). Cellular toxicity was calculated as [dead cell count/(dead cell count + live cell count)] in each image, triplicates were averaged per independent sample, and the mean normalized to baseline cell death in non-treated controls of each experimental replicate.

2.7. Liposome transfection and gene expression analysis

At ~80% confluence, cells were treated with LDS groups at equimolar siRNA content of 200nM in DMEM for 4hr or 24hr. At the indicated transfection time, DMEM was removed, and cells were incubated an additional 24h in VascuLife growth medium before collection for quantitative polymerase chain reaction (qPCR). All qPCR reagents were obtained from ThermoFisher Scientific unless otherwise noted. Total RNA was isolated using Ambion Paris Kit according to manufacturer's instructions, and 200ng (VSMC) or 100ng (VEC) was converted to cDNA using the High Capacity RNA-to-cDNA Master Mix. Two microliters of cDNA transcripts were amplified by qPCR using TaqMan® Gene Expression Master Mix and predesigned TaqMan Gene Expression Assays specific for human GAPDH on the StepOne PCR system (Applied Biosystems, Foster City, CA, USA). The comparative cycle threshold method was used to determine relative quantity of GAPDH mRNA in LDS treated samples compared with non-treated controls (NC). All mRNA amounts were normalized to 18S ribosomal RNA as an endogenous control.

2.8. Statistical Analysis

All data are reported as mean \pm SEM. Statistical analyses were performed using Student's *t*-test or one-way ANOVA and a post-hoc Student-Newman-Keuls test using SigmaStat 3.5 software (Systat Software, Inc., San Jose, CA). Probability (*P*) values ≤ 0.05 were considered to be significant.

3. Results and Discussion

3.1. Prospects of DAG and PS for enhancing cell delivery

DAG is a prime candidate to test our theory that signaling lipids could be used to enhance delivery in the targeting of nanocarriers. DAG is a crucial lipid operator of vesicular biological correspondences, modulating the body's use of lysosomes and lipidic vesicles to communicate and shuttle cargo both intercellularly and intracellularly (Augustin et al., 2001; Johnson et al., 2007). Moreover, tight control of signaling lipid abundance seems to be crucial for smooth muscle cell function (Mason and Jacob, 2003; Ohanian et al., 1998), and there is evidence to suggest that cell-specific proteomes will have preference for certain membrane compositions (Cho and Stahelin, 2005; Niphakis et al., 2015).

Differential lipid expression is a well-established feature of cells and part of what determines their function. Moreover, when healthy cells become diseased or injured, such as tumors or the cardiac tissues of heart attack patients, their fatty acid and phospholipid composition changes (Baenke et al., 2013; Luostarinen et al., 1993). Given the diversity of lipids and their cellular importance, tailoring the natural signaling lipid content of liposomes to generate specificity and/or increase delivery efficacy arises as an intriguing strategy. In particular, DAG has been implicated to have roles in Alzheimer's disease, lymphocyte activity, immunological signal transduction, liver disease, and many forms of cancer (Chan et al., 2012; Wood et al., 2015; Chauveau et al., 2014; Quann et al., 2009; Gorden et al., 2011; (Griner and Kazanietz, 2007). Protein Kinase C (PKC) is activated by DAG and has been hotly investigated for its role as a tumor suppressor (Antal et al., 2015). PKC isozymes have many other roles and are under-expressed in erythrocyte membranes of hypertensive patients (Escriba et al., 2003). DAG regulates a host of other proteins crucial to countless cellular functions both healthy and pathological. Among these other DAG-binding proteins is protein kinase D (PKD), which governs cellular pathologies including cardiac hypertrophy and tumor metastasis (Durand et al., 2016; Wang, 2006).

PS, an anionic cofactor for DAG's binding of many proteins (Stahelin et al., 2005) and an important

apoptotic lipid (Zwaal et al., 2005), was tested alongside DAG. PS is the lone example of a rationally selected natural lipid already reported as part of a commercially available liposomal nanodrug (Bulbake et al., 2017). PS can be used to target liposomes to macrophages (Anderson et al., 2010), which are drawn to PS when flipped to outer-leaflets of apoptotic cells. Apart from this example, lipid signaling has not been used to target LDSs, to our knowledge. In our system, if the mechanism of DAG-potentiated increases in cell association involves DAG's affinity for proteins on cell surfaces, the inclusion of PS within LDSs could also enhance interactions with proteins that bind DAG and PS jointly.

Examples of successful deviations from traditional phosphatidylcholine (PC)-vesicles include the inclusion of phosphatidylglycerol (PG), phosphatidylethanolamine (PE) and the cationic lipid dioleyloxypropyltrimethylammonium (DOTAP) (Bulbake et al., 2017). DOTAP is essentially dioleoyl PC, but the phosphate group is replaced by a cationic trimethyl ammonium at its *sn*-1 position. Sphingomyelin (SM) may also be exchanged for PC to create SM + cholesterol liposomes, termed Optisomes® (Pillai and Ceballos-Coronel, 2013), which are well-established alternatives to PEG-PC liposomes for extended circulation, evasion of the RES, and the passive delivery of drug cargo (Webb et al., 1995). Other lipid add-ins to LDSs include fatty glycerides such as triolein or tricaprylin, which afford opportunities to control LDS stability for specific applications (Gluck and Metcalfe, 2002; Hartrick and Hartrick, 2008). PG, PE and triglycerides are similarly incorporated as favorable structural components (Walsh et al., 1998; Zylberberg and Matosevic, 2016), but not for their abilities to increase cellular association of LDSs. To our knowledge, DAG species are unexplored as structural or functional components of liposomal nanodrugs.

3.2. Liposome Formulations

This work builds upon our previous efforts to develop LDSs, using CPP-modified neutral stealth liposomes, as molecular nanocarriers for gene therapeutics (Fisher et al., 2017). The previous work utilized liposomes containing 10mol% PEG-2000-PE and 10mol% CPP octa-arginine containing a stearate lipid chain for membrane anchoring (R8-stearate; Figure 1). Rhodamine-PE at 0.1mol% (Rhod-PE) was additionally incorporated into liposomes as a fluorescent label to detect cellular delivery via fluorescence microscopy. The remaining 80 mol% of the liposomes were composed of a 7:3 mixture of DOPC and cholesterol. Here, these formulations were modified by substituting the 7:3 PC/cholesterol with DAG and/or PS at gradient mol%, while keeping all other constituents constant, to determine their effect on cell infiltration and delivery (Figure 2). Details of liposome composition for initial cell association studies can be found in supplementary information Table S1. Control samples were simple PEGylated lipoparticles

with no R8 or DAG/PS addition (PLPs), PEGylated lipoparticles with R8 but no DAG/PS (R8), and 20mol% PS with no R8 (P20N). Liposomes labeled ‘D’ and ‘P’, included the indicated percentages of DAG and PS, respectively.

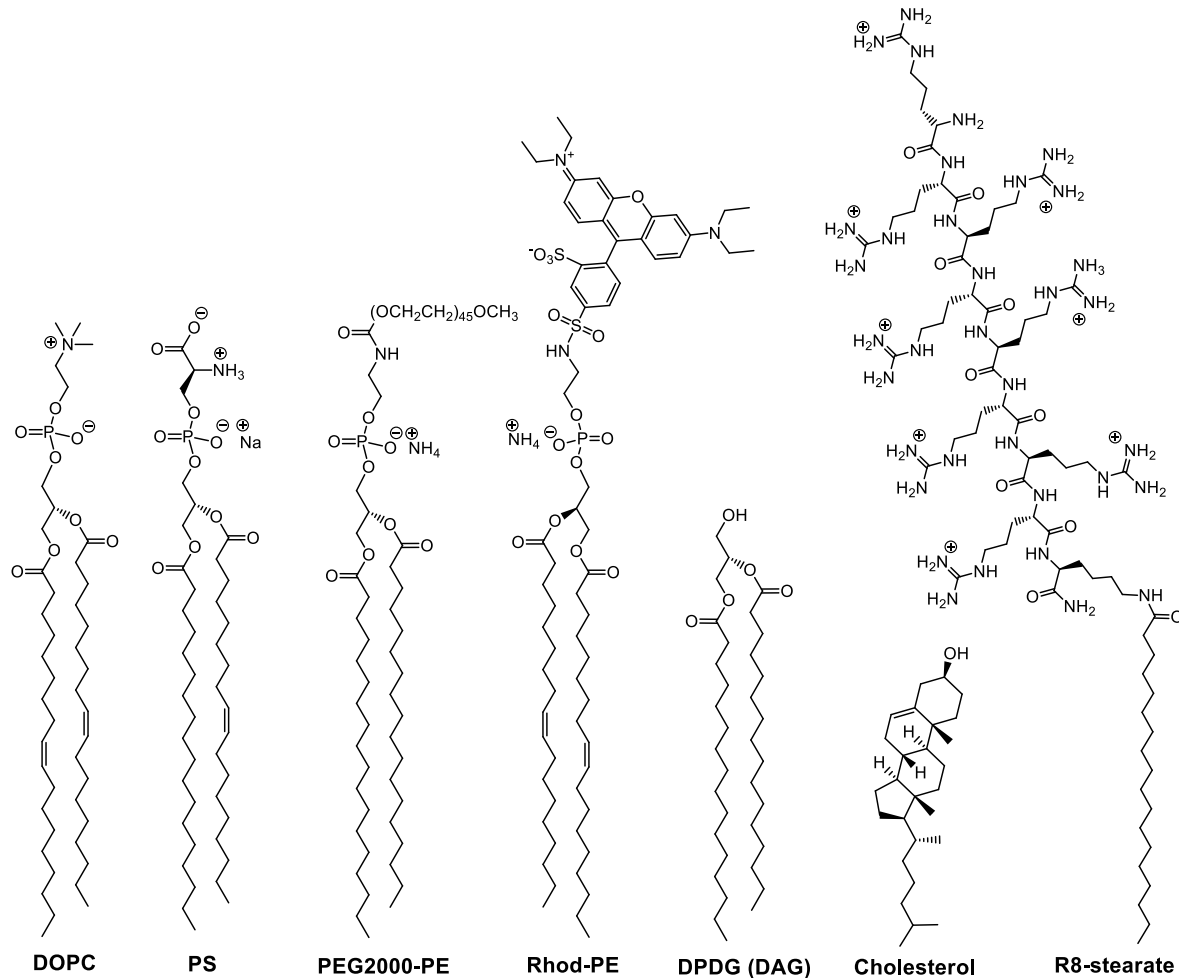


Figure 1: Structures of lipid constituents used for in LDS formulations. 1,2-Dioleoyl-*sn*-glycero-3-phosphocholine (DOPC) is our bulk lipid. Dipalmitoyl DAG and PEG-PE were used. PS was derived naturally from porcine brain tissue and its most abundant form is shown with one palmitic and one oleic tail. Rhodamine-PE (Rhod-PE) is dioleoyl.

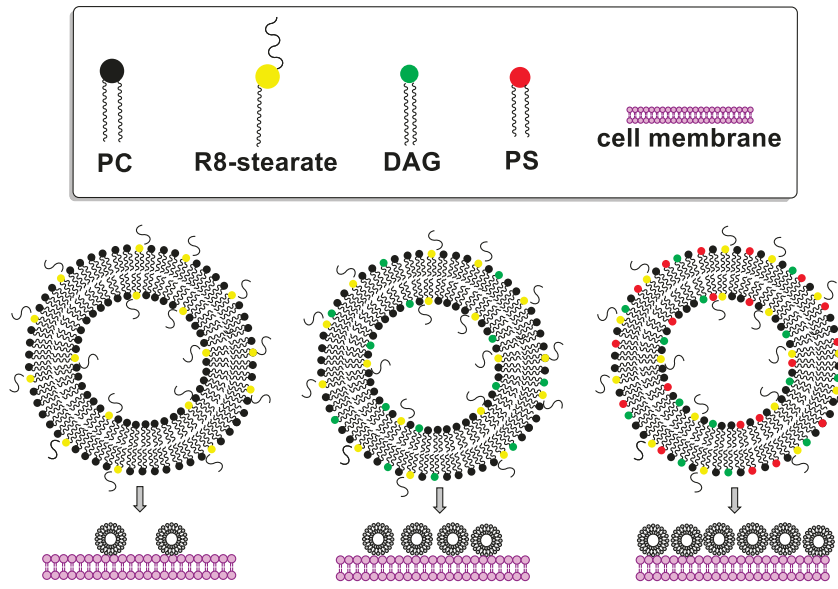


Figure 2: A schematic representation of DAG and/or PS potentiating the cellular association of an R8-LDS. Bulk lipid content also includes cholesterol in a 3:7 ratio with PC, which was reduced to accommodate DAG and/or PS. All liposomes contained equal percentages of PEG-PE and Rhod-PE as well (not shown here). The structures of all liposomal constituents are presented in Figure 2 and details of percent composition of all liposomal formulations can be found in supplementary information Tables S1 and S2.

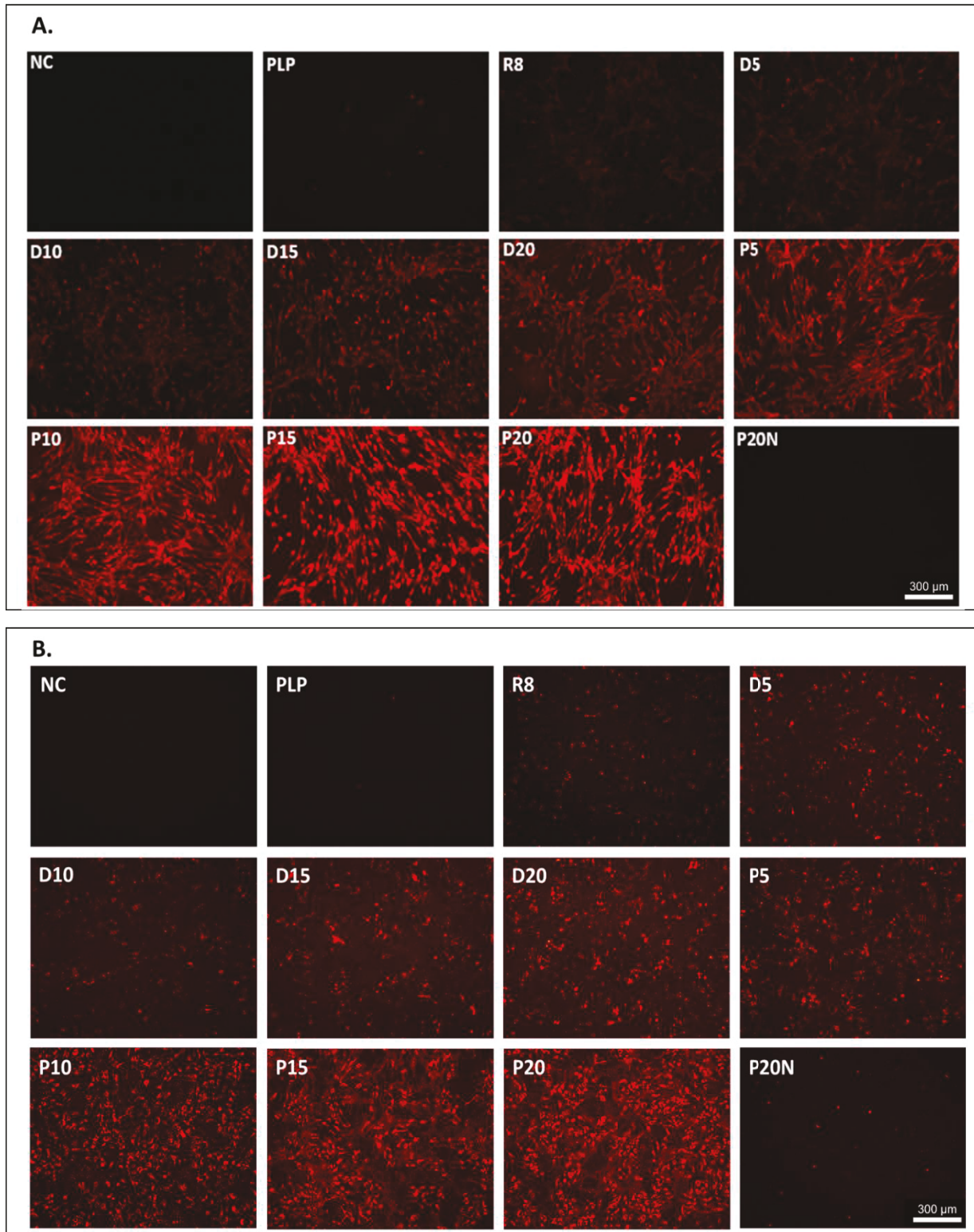


Figure 3: Representative fluorescent microscopy images showing (A.) increased VSMC association and (B.) increased VEC association of liposomes with increasing signaling lipid content. Table S1 provides detailed compositions for each treatment type.

3.2. LDS cell association to VSMCs and VECs potentiated individually by DAG or PS

The results of multiple replicates were quantified based on the percentage of DAG or PS, with both indicating a reproducible enhancement in cell association/entry. As association increases, so too does the total fluorescence of cells, which suggests that liposomes are entering the cell and the Rhod-PE becomes a bilayer component of target cells. Three washes precede microscopy and association quantification, further precluding mere LDS adherence to target cells (rather than entry) as the root of increased fluorescence.

Here, individual DAG or PS incorporation differentially increased vascular cell association of LDSs incorporating R8 alone. Specifically, as %PS increased from the R8 treatment group an exponential increase in cell association was observed, with PS \geq 10mol% and PS \geq 15mol% increased over all other groups in VSMCs and VECs, respectively (Figures 3 and 4). It should be noted here that the percentages of DAG and PS are based off of the molar percentages of these lipids included within the lipid mixture prior to the extrusion process by which liposomes are formed. These results were remarkably consistent, suggesting PS incorporation into the nanocarrier architectures is a promising strategy for potentiating cellular association. While VSMC and VEC association began to drop at levels greater than 10mol% and 15mol% PS, respectively, a linear increase was observed with increasing DAG, but to a lesser degree. The disparity of these results when comparing DAG-only vs. PS-only treatment groups is intriguing, and suggests that signaling lipids could present strategic opportunities to tune the associations of LDSs. An additional control with 20mol% PS and no R8 (P20N) demonstrated the incorporation of signaling lipids alone is not sufficient to enhance LDS delivery, but rather a viable strategy to support the specificity and utility of CPP-modified LDS formulations.

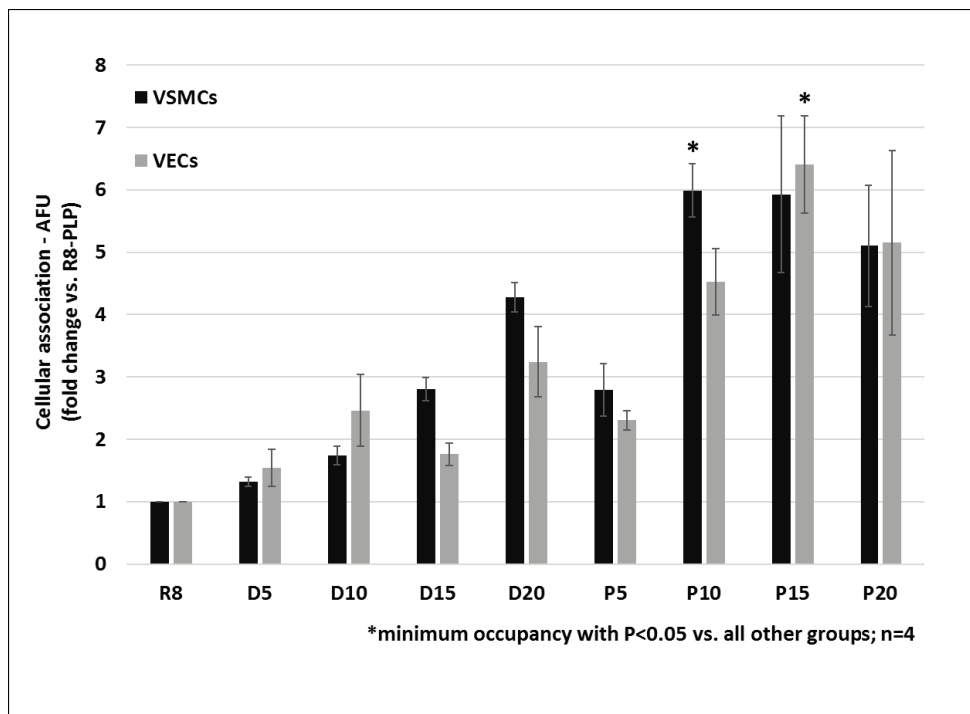


Figure 4: Quantified cell association data from VSMC and VEC experiments. Individual DAG or PS incorporation differentially increased vascular cell association of R8, with PS \geq 10mol% and PS \geq 15mol% increased over all other groups in VSMCs and VECs, respectively. Error bars indicate standard error based on 4 replicates.

3.3. Combinatorial incorporation of DAG with PS further potentiated VSMC but not VEC association

Having observed increases in cell association driven individually by both DAG and PS, we next studied combinations of these to probe for potential synergy. These experiments were performed in similar fashion to individual DAG and PS studies, with fluorescence microscopy again used to image cell association. The liposome compositions for these samples are shown in Table S2 of the supplementary information, which are based upon the fixing of PS at the optimized mol% for each cell type, while varying DAG at 5-20mol%. With PS fixed at 10mol%, the combinatorial incorporation of DAG further potentiated VSMC association at all tested levels (Figures 5 and 6). However, the incorporation of DAG did not potentiate VEC association above PS at 15mol% alone (Figures 5 and 6). This data suggests that PS and DAG are capable of imbuing LDSs with tunable targeting capabilities. More studies are required, but there appear to be disparate trends between DAG and PS as we move from VSMCs to VECs, leaving the possibility where PS-LDS could selectively target only one cell type while DAG-LDS could target the other upon further optimization.

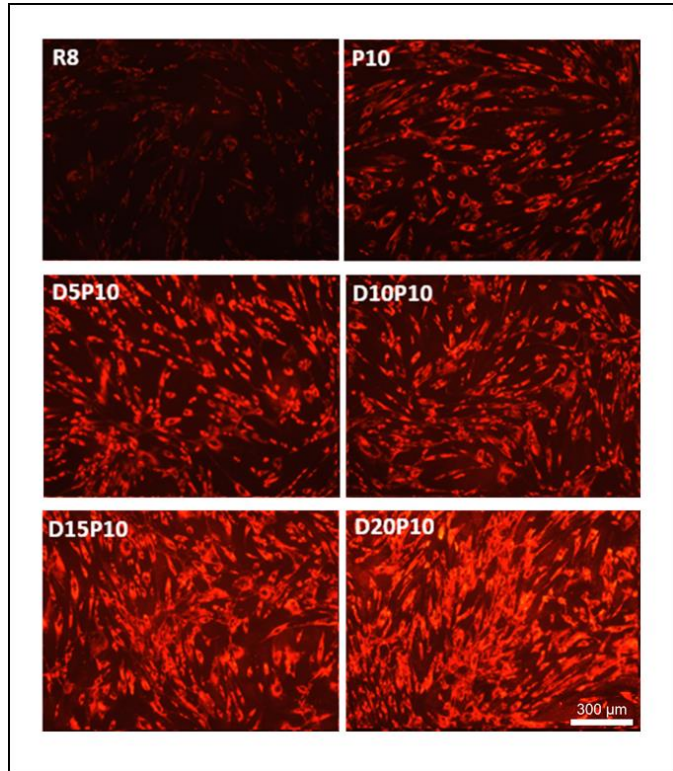


Figure 5: Representative fluorescent microscopy images showing increased VSMC association of DAG+PS combinatorial LDS formulations. Table S2 provides detailed compositions for each treatment type.

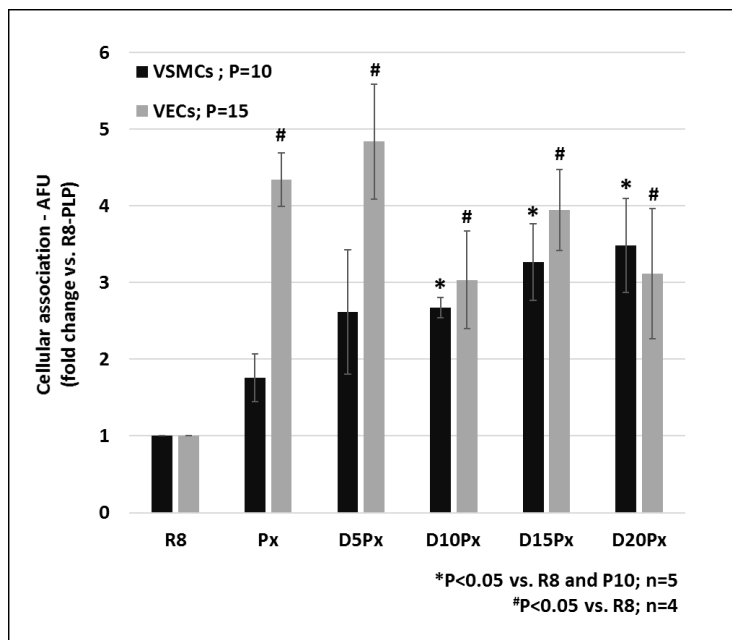


Figure 6: Quantified cell association data using combinatorial formulations of DAG/PS. With PS fixed at 10mol%, the combinatorial incorporation of DAG further potentiated VSMC association at all tested mol%, but did not potentiate VEC association above PS at 15mol% alone. Error bars indicate standard error based on 4-5 replicates.

3.4. Incorporation of DAG into the LDS architecture decreased VSMC cytotoxicity, but conveyed no protective effect in VECs

Exposure of VSMC and VEC to LDSs with R8 but no DAG or PS modification resulted in approximately 2% cell death above basal cell toxicity in culture. The incorporation of signaling lipids into the R8 architecture had no deleterious effect on LDS-mediated cytotoxicity. In fact, PS alone at the level determined to be optimal for LDS association of each cell type had no effect. However, the combinatorial modification with DAG incorporation at $\leq 15\text{mol}\%$ significantly decreased R8-mediated toxicity in VSMC, but demonstrated no protective effect in VECs (Figure 7). Of note, we observed morphological changes in cell membranes in treatment groups with very high cellular association measurements, but the cytotoxicity profiles of these groups were almost negligible. A potential explanation could be that the increased uptake of DAG/PS LDSs leads to incorporation of DAG and PS into the cell membranes, altering bilayer shape. Another possibility is that since DAG and PS play signaling roles in cells, the delivery of these particular lipids could augment cellular processes. However, these lipids are also modified by a number of biosynthetic pathways by which cells would be expected to quickly equilibrate to normal lipid distributions, which is a potential benefit of using naturally existing lipids. While the level of LDS-mediated cytotoxicity demonstrated here is minimal in all conditions, any modifications to the nanocarrier architecture that can improve the liposome biocompatibility profile points to an easier path for pre-clinical advancement of the system and increased translational potential overall. Furthermore, the differential effect seen between cell types further supports the idea that liposomal membranes can be mimetically tuned for cell-type specificity and targeting.

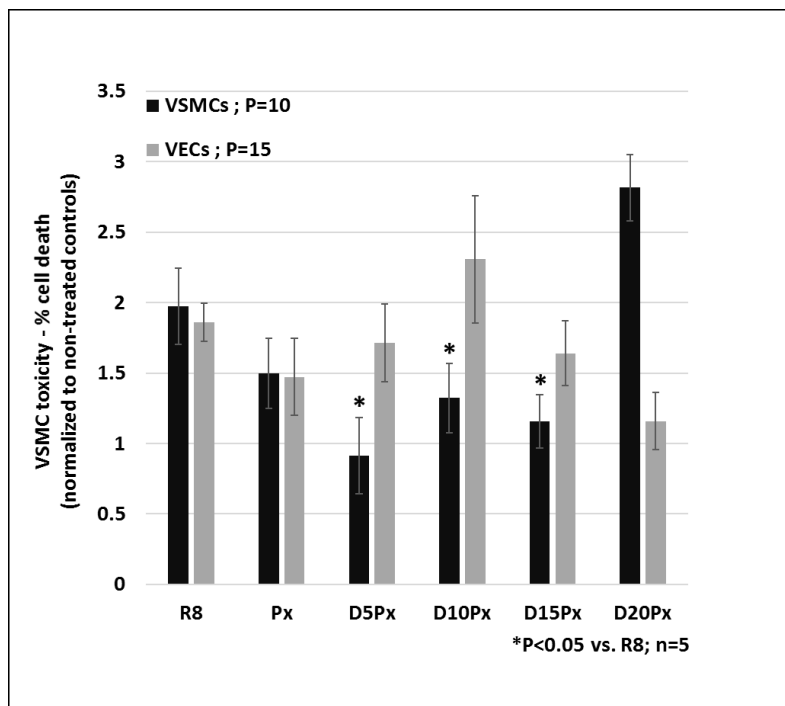


Figure 7: Quantified cytotoxicity data of DAG/PS liposomes. DAG \leq 15mol% significantly decreased R8-mediated toxicity in VSMC, but demonstrated no protective effect in VECs. Error bars indicate standard error based on 5 replicates.

3.5. Effective gene silencing is not enhanced by cell mimetic LDS tuning.

Based on our previous work and correlations between cell association and gene transfection, we anticipated that our novel LDS formulations would achieve significantly higher delivery profiles than R8-only controls. Surprisingly, transfection of VSMC with the DAG/PS modified liposome did not significantly increase targeted gene silencing above R8, when using our previously established standard 4hr transfection procedure (Figure 8A). Additional transfection timelines profiles were then assayed for efficacy validation, using the empirically defined DAG/PS formulations that were determined optimal for each cell type. However, even transfection at 24hr did not significantly increase targeted gene silencing above R8 transfection in VSMCs or VECs (Figure 8B). As yet, our results suggest that DAG/PS incorporation into the LDS architecture does not contribute to enhanced siRNA function, despite the indisputable benefit of enhanced cellular association and cell-type specific mimetic tuning. Possible explanations for this disparate finding could include that our established LDS platform with R8 alone is already effective in siRNA delivery and function in terms of the threshold for experimental in vitro validation. Additional studies could involve assaying the effect of DAG/PS modification while carrying molecular cargo for the targeting of a less constitutive gene family with more strenuous knockdown profiles. Additionally, other cargo materials should be investigated for their increased efficacy besides siRNA. It stands to reason that less stringent therapeutic modalities (in terms of targeting specificity and

threshold) may glean a greater benefit from the demonstrated enhanced LDS cellular association.

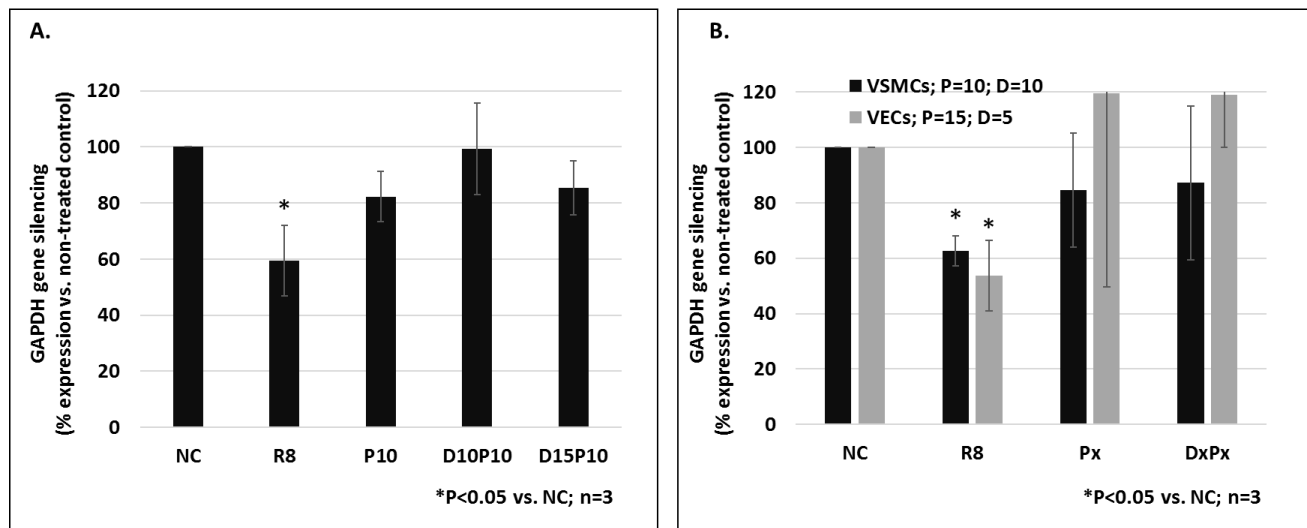


Figure 8: Quantified GAPDH gene silencing data using optimal DAG/PS liposomes formulations for each cell type. A. Transfection of VSMCs with the DAG/PS modified liposomes did not increase targeted gene silencing above R8 at 4hr. **B.** After 24hr transfaction, DAG/PS modified liposomes did not increase targeted gene silencing above R8 in either cell type. Error bars indicate standard error based on 3 replicates.

3.6. Liposomal characterization of DAG/PS modified liposomes

The demonstrable increases in association of our vesicles by adding DAG and/or PS was a promising result at the outset of our project. However, the LDS platform P must retain its membrane stability and the ability to encapsulate genetic cargo when the signaling lipids are added if they are to be a clinically viable targeting strategy. Therefore, standard nanoparticle characterization studies were performed to investigate these properties using formulations with high levels of signaling lipid incorporation. Dynamic light scattering (DLS) was used to measure average nanoparticle size and the homogeneity of the nanoparticle populations, measured as polydispersity index (PDI). DLS data confirmed that our liposomes have consistent integrity when formed with encapsulated siRNA cargo. Figures 9A and B show that liposome stability profiles were not significantly different among groups, with all groups measuring ~60-70nm in diameter and PDI consistently at or below 0.2. Previous in vivo studies using liposome-mediated gene therapy have shown neutral liposomes <100 nm in diameter to have increased circulation half-life, putting our LDS well within the desired quality attributes of biocompatible nanoparticles for translational

therapy. Although PDIs rise with the addition of DAG and/or PS compared to R8 only, the observed diameter reliability is within tolerable ranges for such a complex LDS.

Encapsulation efficiency experiments demonstrated that our DAG/PS-modified LDSs retain their ability to secure genetic cargo for therapeutic applications. siRNA encapsulation was measured by rupturing the assembled liposome membranes by detergent denaturation to release encapsulated and/or entrapped siRNA cargo for fluorescent labeling and quantification via Ribogreen analysis. As can be seen in Figure 9C, we found that the incorporation of DAG/PS within the LDS did not affect the ability of the liposomes to encapsulate or entrap nucleic acid cargo, with ~50-65% of total siRNA retention in all nanoparticle groups.

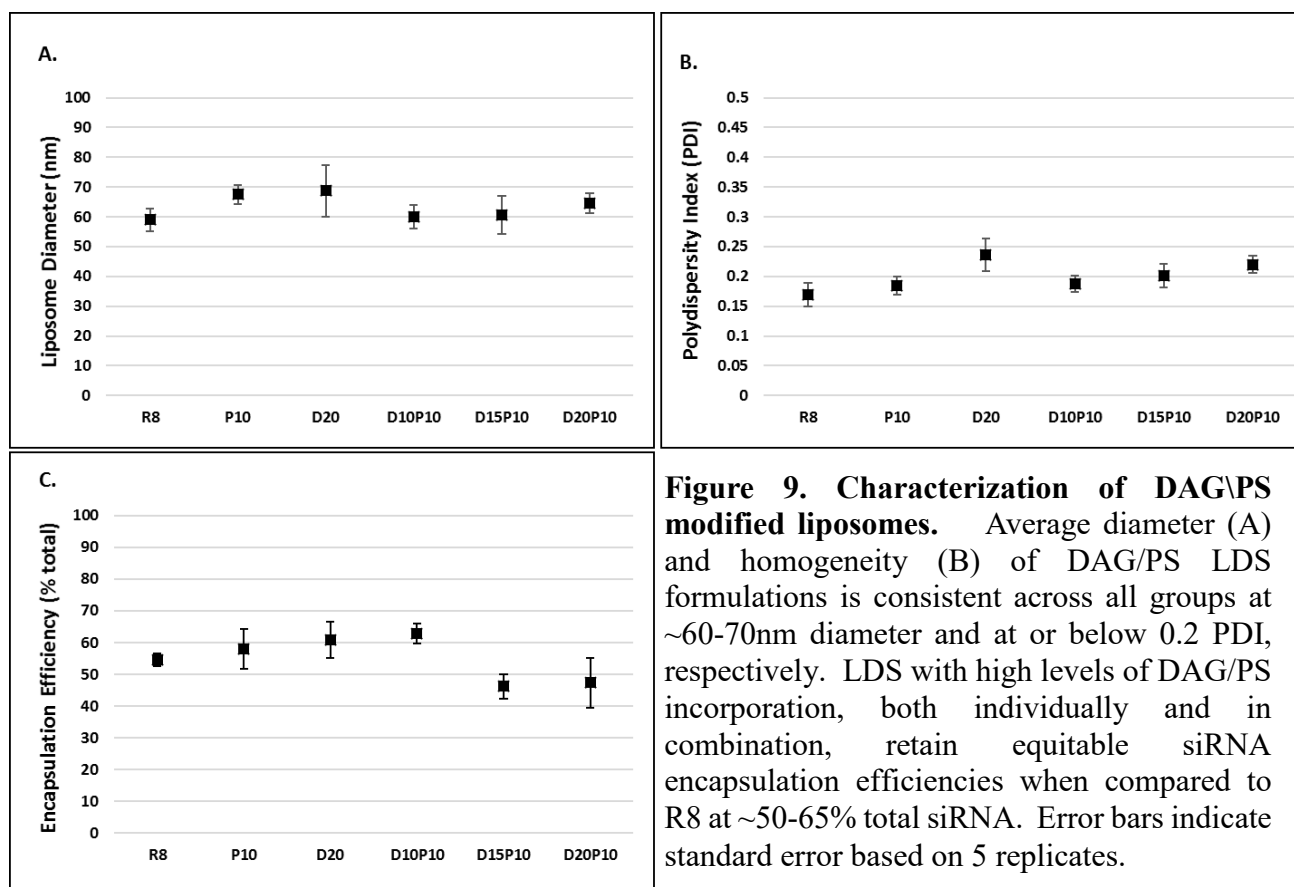


Figure 9. Characterization of DAG\PS modified liposomes. Average diameter (A) and homogeneity (B) of DAG/PS LDS formulations is consistent across all groups at ~60-70nm diameter and at or below 0.2 PDI, respectively. LDS with high levels of DAG/PS incorporation, both individually and in combination, retain equitable siRNA encapsulation efficiencies when compared to R8 at ~50-65% total siRNA. Error bars indicate standard error based on 5 replicates.

4. Conclusions

We have shown that using the lipid second messengers DAG and PS is a viable, natural strategy towards increasing liposomal nanodrug efficacies in a membrane-mimetic, tunable manner. There is evidence here to support that this strategy could be further optimized to enhance cell-type specificity.

Though we have not yet demonstrated complete selectivity, the utility of these lipids to increase treatment efficacies is already apparent, even at this early stage of experimentation. The results so far suggest that continued exploration of lipid-guided LDSs could uncover formulations that can indeed target one cell type over the other with consistency. These discriminant effects would be ideal for our applications, but the utility of signaling lipids in the nanodrug architectures to provide universal increases in delivery efficacy also remains a worthwhile discovery.

As discussed in the introduction, this is an intuitive strategy. Nonetheless, the work we describe here is novel. Some studies have broached this concept, such as experimentation with raft-like LDSs for HIV-1 treatment (Gomara et al., 2017). DAG and PS have both been widely studied for their ability to promote fusion between vesicles (Goldberg et al., 1994; Wilschut et al., 1980). Added fusogenic tendencies could be a key component driving enhanced delivery using liposomes incorporating DAG and/or PS in LDS architectures. PS is envisioned to work electrostatically, given its negative charge, while DAG is known to be a key factor in promoting vesicular communications that require fission and fusion of smaller lipid vesicles sent intra/extracellularly or at synaptic gaps (Quann et al., 2009; Sarri et al., 2011; Spitaler et al., 2006). At the least, increased fusogenic behavior of liposomes with elevated DAG/PS content should be considered a contributing variable to the cell association studies described herein. Lipid-protein and lipid-lipid interactions between liposomes and cell surfaces remain plausible explanations for the dose-dependent increases in association of DAG and/or PS-containing liposomes that occur disparately between types of cells/LDS formulations. This raises the possibility that signaling lipids could be effective for active targeting of overly abundant proteins selectively expressed in specific cell types. Overall, this project demonstrates that natural lipids such as DAG and PS present facile solutions to increasing the cellular association of liposomal nanocarriers, and opens the door to investigating myriad permutations of natural lipids that may control liposome cell association.

Acknowledgments

We acknowledge partial support of this work from a collaborative POG seed grant from the University of Tennessee Graduate School of Medicine/University of Tennessee-Knoxville, and from the National Science Foundation Grant under award number DMR-1807689.

References

Alam, S., Mattern-Schain, S., and Best, M. 2017. Targeting and triggered release using lipid-based supramolecular assemblies as medicinal nanocarriers. In *Comprehensive Supramolecular Chemistry II*, J.L. Atwood, ed. (Oxford: Elsevier), pp. 329-364.

Anderson, P.M., Tomaras, M., and McConnell, K., 2010. Mifamurtide in osteosarcoma--a practical review. *Drugs Today* 46, 327-337.

Antal, C.E., Hudson, A.M., Kang, E., Zanca, C., Wirth, C., Stephenson, N.L., Trotter, E.W., Gallegos, L.L., Miller, C.J., Furnari, F.B., *et al.*, 2015. Cancer-associated protein kinase C mutations reveal kinase's role as tumor suppressor. *Cell* 160, 489-502.

Augustin, I., Korte, S., Rickmann, M., Kretzschmar, H.A., Südhof, T.C., Herms, J.W., and Brose, N., 2001. The Cerebellum-Specific Munc13 Isoform Munc13-3 Regulates Cerebellar Synaptic Transmission and Motor Learning in Mice. *J. Neurosci.* 21, 10.

Baenke, F., Peck, B., Miess, H., and Schulze, A., 2013. Hooked on fat: the role of lipid synthesis in cancer metabolism and tumour development. *Dis. Model. Mech.* 6, 1353-1363.

Barenholz, Y., 2012. Doxil(R)--the first FDA-approved nano-drug: lessons learned. *J. Control. Release* 160, 117-134.

Bulbake, U., Doppalapudi, S., Kommineni, N., and Khan, W., 2017. Liposomal Formulations in Clinical Use: An Updated Review. *Pharmaceutics* 9.

Chan, R.B., Oliveira, T.G., Cortes, E.P., Honig, L.S., Duff, K.E., Small, S.A., Wenk, M.R., Shui, G., and Di Paolo, G., 2012. Comparative lipidomic analysis of mouse and human brain with Alzheimer disease. *J. Biol. Chem.* 287, 2678-2688.

Chauveau, A., Le Floc'h, A., Bantilan, N.S., Koretzky, G.A., and Huse, M., 2014. Diacylglycerol kinase alpha establishes T cell polarity by shaping diacylglycerol accumulation at the immunological synapse. *Sci. Signal.* 7, ra82.

Cho, W., and Stahelin, R.V., 2005. Membrane-protein interactions in cell signaling and membrane trafficking. *Annu. Rev. Biophys. Biomol. Struct.* 34, 119-151.

Dicheva, B.M., ten Hagen, T.L.M., Seynhaeve, A.L.B., Amin, M., Eggermont, A.M.M., and Koning, G.A., 2015. Enhanced Specificity and Drug Delivery in Tumors by cRGD - Anchoring Thermosensitive Liposomes. *Pharm. Res.* 32, 3862-3876.

Durand, N., Borges, S., and Storz, P., 2016. Protein Kinase D Enzymes as Regulators of EMT and Cancer Cell Invasion. *J. Clin. Med.* 5.

Escriba, P.V., Sanchez-Dominguez, J.M., Alemany, R., Perona, J.S., and Ruiz-Gutierrez, V., 2003. Alteration of lipids, G proteins, and PKC in cell membranes of elderly hypertensives. *Hypertension* 41, 176-182.

Fisher, R.K., Mattern-Schain, S.I., Best, M.D., Kirkpatrick, S.S., Freeman, M.B., Grandas, O.H., and Mountain, D.J.H., 2017. Improving the efficacy of liposome-mediated vascular gene therapy via lipid surface modifications. *J. Surg. Res.* 219, 136-144.

Gluck, R., and Metcalfe, I.C., 2002. New technology platforms in the development of vaccines for the future. *Vaccine* 20 Suppl 5, B10-16.

Goldberg, E.M., Lester, D.S., Borchardt, D.B., and Zidovetzki, R., 1994. Effects of diacylglycerols and Ca²⁺ on structure of phosphatidylcholine/phosphatidylserine bilayers. *Biophys. J.* 66, 382-393.

Gomara, M.J., Perez-Pomeda, I., Gatell, J.M., Sanchez-Merino, V., Yuste, E., and Haro, I., 2017. Lipid raft-like liposomes used for targeted delivery of a chimeric entry-inhibitor peptide with anti-HIV-1 activity. *Nanomedicine* 13, 601-609.

Gorden, D.L., Ivanova, P.T., Myers, D.S., McIntyre, J.O., VanSaun, M.N., Wright, J.K., Matrisian, L.M., and Brown, H.A., 2011. Increased diacylglycerols characterize hepatic lipid changes in progression of human nonalcoholic fatty liver disease; comparison to a murine model. *PLoS One* 6, e22775.

Griner, E.M., and Kazanietz, M.G., 2007. Protein kinase C and other diacylglycerol effectors in cancer. *Nat. Rev. Cancer* 7, 281-294.

Hartrick, C.T., and Hartrick, K.A., 2008. Extended-release epidural morphine (DepoDur): review and safety analysis. *Exp. Rev. Neurother.* 8, 1641-1648.

Johnson, Joanne E., Goulding, Rebecca E., Ding, Z., Partovi, A., Anthony, Kira V., Beaulieu, N., Tazmini, G., Cornell, Rosemary B., and Kay, Robert J., 2007. Differential membrane binding and diacylglycerol recognition by C1 domains of RasGRPs. *Biochem. J.* 406, 223-236.

Kanapathipillai, M., Brock, A., and Ingber, D.E., 2014. Nanoparticle targeting of anti-cancer drugs that alter intracellular signaling or influence the tumor microenvironment. *Adv. Drug Deliv. Rev* 79-80, 107-118.

Landesman-Milo, D., and Peer, D., 2016. Transforming Nanomedicines From Lab Scale Production to Novel Clinical Modality. *Bioconjugate Chem.* 27, 855-862.

Luostarinen, R., Boberg, M., and Saldeen, T., 1993. Fatty acid composition in total phospholipids of human coronary arteries in sudden cardiac death. *Atherosclerosis* 99, 187-193.

Mason, R.P., and Jacob, R.F., 2003. Membrane microdomains and vascular biology: emerging role in atherogenesis. *Circulation* 107, 2270-2273.

Niphakis, M.J., Lum, K.M., Cognetta, A.B., 3rd, Correia, B.E., Ichu, T.A., Olucha, J., Brown, S.J., Kundu, S., Piscitelli, F., Rosen, H., et al., 2015. A Global Map of Lipid-Binding Proteins and Their Ligandability in Cells. *Cell* 161, 1668-1680.

Ohanian, J., Liu, G., Ohanian, V., and Heagerty, A.M., 1998. Lipid second messengers derived from glycerolipids and sphingolipids, and their role in smooth muscle function. *Acta Physiol. Scand.* 164, 533-548.

Pattini, B.S., Chupin, V.V., and Torchilin, V.P., 2015. New Developments in Liposomal Drug Delivery. *Chemical Rev.* 115, 10938-10966.

Pillai, G., and Ceballos-Coronel, M.L., 2013. Science and technology of the emerging nanomedicines in cancer therapy: A primer for physicians and pharmacists. *SAGE Open Medicine* 1, 2050312113513759.

Quann, E.J., Merino, E., Furuta, T., and Huse, M., 2009. Localized diacylglycerol drives the polarization of the microtubule-organizing center in T cells. *Nat. Immunol.* 10, 627-635.

Sarri, E., Sicart, A., Lazaro-Diequez, F., and Egea, G., 2011. Phospholipid synthesis participates in the regulation of diacylglycerol required for membrane trafficking at the Golgi complex. *J. Biol. Chem.* 286, 28632-28643.

Saw, P.E., Kim, S., Lee, I.H., Park, J., Yu, M., Lee, J., Kim, J.I., and Jon, S., 2013. Aptide-conjugated liposome targeting tumor-associated fibronectin for glioma therapy. *J. Mater. Chem. B* 1, 4723-4726.

Spitaler, M., Emslie, E., Wood, C.D., and Cantrell, D., 2006. Diacylglycerol and protein kinase D localization during T lymphocyte activation. *Immunity* 24, 535-546.

Stahelin, R.V., Wang, J., Blatner, N.R., Rafter, J.D., Murray, D., and Cho, W., 2005. The origin of C1A-C2 interdomain interactions in protein kinase Calpha. *J. Biol. Chem.* 280, 36452-36463.

Walsh, T.J., Hiemenz, J.W., Seibel, N.L., Perfect, J.R., Horwith, G., Lee, L., Silber, J.L., DiNubile, M.J., Reboli, A., Bow, E., *et al.*, 1998. Amphotericin B lipid complex for invasive fungal infections: analysis of safety and efficacy in 556 cases. *Clin. Infect. Dis.* 26, 1383-1396.

Wang, Q.J., 2006. PKD at the crossroads of DAG and PKC signaling. *Trends Pharmacol. Sci.* 27, 317-323.

Webb, M.S., Harasym, T.O., Masin, D., Bally, M.B., and Mayer, L.D., 1995. Sphingomyelin-cholesterol liposomes significantly enhance the pharmacokinetic and therapeutic properties of vincristine in murine and human tumour models. *Brit. J. Cancer* 72, 896-904.

Wilschut, J., Duzgunes, N., Fraley, R., and Papahadjopoulos, D., 1980. Studies on the mechanism of membrane fusion: kinetics of calcium ion induced fusion of phosphatidylserine vesicles followed by a new assay for mixing of aqueous vesicle contents. *Biochemistry* 19, 6011-6021.

Wood, P.L., Medicherla, S., Sheikh, N., Terry, B., Phillipps, A., Kaye, J.A., Quinn, J.F., and Woltjer, R.L., 2015. Targeted Lipidomics of Frontal Cortex and Plasma Diacylglycerols (DAG) in Mild Cognitive Impairment (MCI) and Alzheimer's Disease: Validation of DAG Accumulation Early in the Pathophysiology of Alzheimer's Disease. *J. Alzheimer's Dis.* : JAD 48, 537-546.

Ylä-Herttula, S., and Martin, J.F., 2000. Cardiovascular gene therapy. *Lancet* 355, 213-222.

Zwaal, R.F., Comfurius, P., and Bevers, E.M., 2005. Surface exposure of phosphatidylserine in pathological cells. *Cell. Molec. Life Sci.* 62, 971-988.

Zylberberg, C., and Matosevic, S., 2016. Pharmaceutical liposomal drug delivery: a review of new delivery systems and a look at the regulatory landscape. *Drug. Deliv.* 23, 3319-3329.